

OPEN

A Hyper-Crosslinked Carbohydrate Polymer Scaffold Facilitates Lineage Commitment and Maintains a Reserve Pool of Proliferating Cardiovascular Progenitors

Jonathan M. Baio, BS,¹ Ryan C. Walden, MS,¹ Tania I. Fuentes, PhD,¹ Charles C. Lee, PhD,² Nahidh W. Hasaniya, MD,³ Leonard L. Bailey, MD,³ Mary K. Kearns-Jonker, PhD¹

Background. Cardiovascular progenitor cells (CPCs) have been cultured on various scaffolds to resolve the challenge of cell retention after transplantation and to improve functional outcome after cell-based cardiac therapy. Previous studies have reported successful culture of fully differentiated cardiomyocytes on scaffolds of various types, and ongoing efforts are focused on optimizing the mix of cardiomyocytes and endothelial cells as well as on the identification of a source of progenitors capable of reversing cardiovascular damage. A scaffold culture that fosters cell differentiation into cardiomyocytes and endothelial cells while maintaining a progenitor reserve would benefit allogeneic cell transplantation. **Methods.** Isl-1 + c-Kit + CPCs were isolated as clonal populations from human and sheep heart tissue. After hyper-crosslinked carbohydrate polymer scaffold culture, cells were assessed for differentiation, intracellular signaling, cell cycling, and growth factor/chemokine expression using real time polymerase chain reaction, flow cytometry, immunohistochemistry, and calcium staining. **Results.** Insulin-like growth factor 1, hepatocyte growth factor, and stromal cell derived factor 1 α paracrine factors were induced, protein kinase B signaling was activated, extracellular signal-regulated kinase phosphorylation was reduced and differentiation into both cardiomyocytes and endothelial cells was induced by scaffold-based cell culture. Interestingly, movement of CPCs out of the G1 phase of the cell cycle and increased expression of pluripotency genes *PLOU5F1* (Oct4) and *T* (Brachyury) within a portion of the cultured population occurred, which suggests the maintenance of a progenitor population. Two-color immunostaining and 3-color fluorescence-activated cell sorting analysis confirmed the presence of both Isl-1 expressing undifferentiated cells and differentiated cells identified by troponin T and von Willebrand factor expression. Ki-67 labeling verified the presence of proliferating cells that remained in situ alongside the differentiated functional derivatives. **Conclusions.** Cloned Isl-1 + c-kit + CPCs maintained on a hyper-cross linked polymer scaffold retain dual potential for proliferation and differentiation, providing a scaffold-based stem cell source for transplantation of committed and proliferating cardiovascular progenitors for functional testing in preclinical models of cell-based repair.

(*Transplantation Direct* 2017;3: e153; doi: 10.1097/TXD.0000000000000667. Published online 13 April, 2017.)

Manipulating the limited regenerative capacity of the human heart through endogenous cardiovascular progenitor cells (CPCs) presents a promising avenue for

cardiovascular repair.¹⁻¹⁰ The transplantation of tissue on supportive structures made of biodegradable materials has been receiving increasing attention.¹¹⁻¹⁴ This transition to a

Received 5 October 2016. Revision requested 27 January 2017.

Accepted 12 February 2017.

¹ Department of Pathology and Human Anatomy, Loma Linda University School of Medicine, Loma Linda, CA.

² Molecular Matrix, Davis, CA.

³ Department of Cardiovascular and Thoracic Surgery, Loma Linda University School of Medicine, Loma Linda, CA.

This work was supported by CIRM Bridges to Stem Cell Research Grant No. TB1-01185 to RW.

Conflict of Interest: Charles Lee of Molecular Matrix, Inc, is the creator of the scaffold used in this research. The remaining authors declare no conflicts of interest.

J.M.B. and R.C.W. contributed equally to this study.

All authors contributed to the analysis and interpretation of data; were involved in revising important intellectual content; approved the final version for publication; and agree to be accountable for all aspects of the work related to the accuracy

and integrity of any part of the work. J.B., R.W., T.F., and M.K.-J. additionally contributed to the design of the work, the drafting of important intellectual content; and data acquisition and analysis. N.H. and L.B. additionally provided tissue from surgical biopsies from which primary cell cultures were obtained. C.L. additionally designed and supplied the scaffold and associated reagents used herein.

Correspondence: Mary Kearns-Jonker, PhD, Division of Human Anatomy, Loma Linda University, 24760 Stewart St, Ste 2215, Loma Linda, CA 92350. (mkearnsjonker@llu.edu).

Copyright © 2017 The Author(s). *Transplantation Direct*. Published by Wolters Kluwer Health, Inc. This is an open-access article distributed under the terms of the Creative Commons Attribution-Non Commercial-No Derivatives License 4.0 (CCBY-NC-ND), where it is permissible to download and share the work provided it is properly cited. The work cannot be changed in any way or used commercially without permission from the journal.

ISSN: 2373-8731

DOI: 10.1097/TXD.0000000000000667

biomimetic, 3-dimensional (3D) apparatus reflects the use of extracellular matrix (ECM)-like conditions.¹² Stem cell-derived cardiac tissues require cellular organization into a functional, 3D structure. These structures facilitate conditions under which growth and differentiation occur because their mechanical properties and topography more closely approximate the *in vivo* environment.¹³ Furthermore, it is possible to develop cardiac tissue with a homogenous distribution of viable cells that express both early transcription factors and cardiomyocyte markers.¹⁴ Tissue printing¹⁴ and harvested organs¹⁵ both have made use of the biomimetic nature of this 3D structural support. The use of patient-derived CPCs can similarly be applied to a 3D environment to promote the development of cardiac tissue.

The use of a cardiac progenitor that has direct cardiomyogenic potential, such as endogenous CPCs, during transplantation may facilitate regeneration. Previous studies that have made use of hematopoietic stem cells^{16,17} and mesenchymal stem cells (MSCs)¹⁸ raised concerns over the myogenic capacity of these cell types. Godier-Furnémont et al,⁴ used MSCs in 1 such study. Although enhanced angiogenic potential was noted, the authors acknowledged that cardiomyogenic differentiation of MSCs was unlikely. Using these progenitor types that are not closely related to cardiac derivatives have resulted in underwhelming clinical trials.¹⁹ Because cardiomyocyte proliferation is limited, it has been challenging to transplant myocytes and achieve tissue-like cell densities.^{12,20,21} Questions regarding the integration of transplanted cells into myocardium^{18,22} and their ability to produce a biologically necessary ratio of cardiomyocytes to vascular tissue have arisen.²³ For example, printing cardiac tissue has produced cardiomyocytes, but whether this method produces additional necessary cardiac derivatives is unknown.¹⁴ A scaffold that promotes the development of an array of cardiac lineages while maintaining a proliferative stem cell reserve could address these barriers to scaffold-based cardiac repair.

Here, we use a hyper-crosslinked carbohydrate polymer scaffold to simultaneously culture and differentiate Isl-1 + c-Kit + CPCs³ that have been derived from human patients and from sheep. We use the sheep model to optimize conditions for transplantation as this model is relevant for application to cardiovascular transplantation in humans. Culturing CPCs using a scaffold attempts to closely approximate the *in vivo* environment of the stem cell.²⁴ We further this work by demonstrating the applicability of both the CPCs presented herein and the scaffold for cardiac tissue regeneration. In doing so, we assessed the ability of this scaffold to influence the cell cycle towards a proliferative state while promoting the differentiation of certain cells within the population. We demonstrate changes in growth factor expression as well as MAPK/extracellular signal-regulated kinase (ERK) and protein kinase B (AKT) signaling after scaffold culture. Because the ovine faithfully reflects cardiac repair mechanisms in humans and represents a useful animal model in which stem cell transplantation conditions can be optimized,^{25,26} we extended this line of inquiry to ovine-derived CPCs. We observed a similar result of cardiac differentiation in some cells on the scaffold while a proportion of cells were maintained in a progenitor state. We report here a scaffold that is suitable for culturing CPCs that can proliferate, as is done in the stem cell niches that maintain a reserve pool of progenitors,

and can differentiate such that specified tissue growth can occur, thereby promoting conditions that support the regeneration of cardiac tissue.

MATERIALS AND METHODS

Institutional Review Board

The institutional review board of Loma Linda University approved the use of tissue that was discarded during cardiovascular surgery, without identifiable private information, for this study with a waiver of informed consent.

Institutional Animal Care and Use Committee

All experimental procedures involving animals were performed within the regulations of the Animal Welfare Act, the National Institutes of Health Guide for the Care and Use of Laboratory Animals, and the Institutional Animal Care and Use Committee of Loma Linda University.

CPC Isolation

CPCs were isolated from surgical biopsies of human neonates (8 days of age) and adults (55-75 years of age) as described previously.²⁷ Right atrial cardiac tissue was mechanically digested and treated with collagenase (Roche Applied Science, Indianapolis, IN) for 2 hours at 37°C. CPCs were cultured in M199-supplemented limiting dilution media at a concentration of 0.8 cells per well to create the clonal populations that were expanded for use in this study. CPCs were similarly isolated and selected from neonatal sheep (9-10 days of age), which were previously characterized.²⁸

Cell Growth on the Scaffold

Before cell seeding, an 8 × 2-mm GroCell-3D hyper-crosslinked carbohydrate polymer scaffold (Molecular Matrix, Davis, CA) with 20- to 80- μ m pores was placed in M199-supplemented growth media at 37°C overnight. The GroCell-3D scaffold is comprised of organic material and has a porosity of 97%. A 20- μ L paste of 2 × 10⁶ CPCs in growth media was placed on top of the culture-soaked scaffold and incubated for 2 hours at 37°C in 5% CO₂ before being placed in growth media. Over 3 weeks, cells that detached from the scaffold were reseeded as needed. Scaffolds were dissolved for subsequent analysis. Dissolution solution (Molecular Matrix) was used to disperse cells with a modified manufacturer's protocol. Briefly, the solution was mixed with M199-supplemented growth media and placed onto the scaffold, before being incubated at 37°C for 90 minutes with agitation. The cells were pelleted at 200g for 8.5 minutes and resuspended for subsequent analysis.

Phosphorylation Assay Using Flow Cytometry

We assessed intracellular signaling by measuring the phosphorylation of ERK and AKT using flow cytometry. Cells were fixed with 4% paraformaldehyde, permeabilized using methanol, and stained using antibodies against p-ERK 1/2 (Thr202/Tyr204; Cell Signaling Technology, Danvers, MA; clone: D13.14.4E), and p-AKT (Ser473; Cell Signaling Technology; clone: D9E). FITC goat anti-rabbit IgG (BD Biosciences San Jose, CA) was used as a secondary antibody. Staining with secondary antibody alone was used to define positive and negative populations. Western blot measurements correspond to those obtained by flow cytometry.²⁹⁻³¹

Stem Cell Progenitor Marker Detection Using Flow Cytometry

We used flow cytometry to measure Isl-1, c-kit, kinase insert domain protein receptor (known as Flk-1) (KDR), and PDGFR α as well as the coexpression of Isl-1 and c-kit. First, cells were labeled to detect KDR and PDGFR α using CD140a-PE (PDGFR α ; clone: 16A1) and PerCP/Cy5.5-conjugated VEGFR2 (also known as FLK1 or KDR) antibodies (Biolegend, San Diego, CA). Isotype controls were matched to the species, isotype, and conjugated fluorophore. These isotypes were used to define negative and positive populations. Isl-1 and c-kit expression was detected in isolation and jointly using DyLight650-conjugated c-kit antibody (Novus Biologicals, Littleton, CO; clone: 2B8) with Alexa Fluor 647-conjugated isotype control (R&D Systems, Minneapolis, MN) and anti-human Isl-1 primary antibody (Abcam, Cambridge, MA; clone: 1H9) with goat, anti-mouse FITC-conjugated secondary antibody (Southern Biotech, Birmingham, AL). Staining with secondary antibody alone used to define positive and negative populations for Isl1. Fluorescently labeled cells were analyzed using MACSquant analyzer (Miltenyi Biotec, Auburn, CA) and FlowJo software (FlowJo, Ashland, OR). Dead cells were gated out using forward-scatter and side-scatter gating.

Dexamethasone Differentiation of CPCs

CPCs were differentiated using dexamethasone.⁶ Briefly, cells were cultured for 6 days in M199-supplemented growth media containing 10-nM dexamethasone. Differentiation markers for cardiomyocytes (troponin T [TropT] and troponin I [TropI]), endothelium (von Willebrand factor [vWF]), and smooth muscle (smooth muscle actin [SMA]) were measured using flow cytometry.

Differentiation Marker Detection Using Flow Cytometry

We used flow cytometry to measure the level of expression of the differentiation markers TropT and vWF, as described previously.²⁷ Lightning-Link Antibody Labeling Kit (Novus Biologicals, Littleton, CO) was used to conjugate rabbit anti-human von-Willbrand factor antibody (Dako, Carpinteria, CA) to FITC and anti-cardiac TropT antibody (Abcam) to PE. Cells were stained with FITC-conjugated vWF and PE-conjugated TropT. Cells were stained with anti-TropI antibody (Millipore, Temecula, CA) and anti-SMA antibody (clone: 1A4; Abcam) before being incubated with PE-conjugated goat anti-mouse secondary antibody (Southern Biotech, Birmingham, AL). To perform 3-color fluorescence-activated cell sorting (FACS) analysis, we used anti-human Isl-1 primary antibody (Abcam), Alexa Fluor647-conjugated anti-human vWF (Novus Biologicals, Littleton, CO; clone: 3E2D10), and PE-conjugated anti-human TropT (Miltenyi Biotec, Auburn, CA). Isotype controls were matched to the species, isotype, and conjugated fluorophore. Isotype controls or secondary antibody alone were used to define positive and negative populations. Optimal antibody concentrations were determined by titration.

Cell cycle analysis using flow cytometry

Cell cycle analysis was conducted using flow cytometry, as previously described.³ Cells were fixed with ethanol and stored for 1 hour at -20°C before being incubated at 37°C with RNase A (0.5 mg/mL; Invitrogen, Carlsbad, CA) for

1 hour. Propidium iodide (Biolegend) was added at a final concentration of 10 $\mu\text{g}/\text{ml}$.

Real-Time Polymerase Chain Reaction

Cells were lysed using Trizol reagent (Invitrogen). Two micrograms of RNA were isolated and used to prepare cDNA with Superscript III (Invitrogen). Real-time polymerase chain reaction (RT-PCR) was run using an IQ5 thermocycler (Bio-rad, Hercules, CA) with β actin as a housekeeping gene. The PCR conditions for all primer pairs (except Bry, Mesp1, and PDGFR α) were: 94°C for 10 minutes and 40 cycles of 94°C for 15 seconds, 52°C for 60 seconds, and 72°C for 30 seconds. The PCR conditions for Bry, Mesp1, and PDGFR α were: 94°C for 10 minutes and 40 cycles of 94°C for 15 seconds, 60°C for 60 seconds, and 72°C for 30 seconds. Primer pairs are listed in Table 1 and were obtained from Integrated DNA Technologies (Coralville, IA).

Calcium flux

Fifty micrograms of fluo4-AM dye (Life Technologies, Carlsbad, CA) was dissolved in pluronic acid and 20% DMSO (Life Technologies) via sonication before being resuspended in M199-supplemented growth media. Cells were incubated with the dye for 1 hour and imaged using a LSM 710 NLO laser-scanning, confocal microscope (Carl Zeiss Microscopy GmbH, Jena, Germany) at a $20\times$ objective. All experiments were conducted at room temperature and in the absence of external electrical stimulation. Images were processed using ImageJ (v.1.49, NIH, <http://imagej.nih.gov/ij>).

Immunohistochemistry

Scaffolds were fixed in 4% paraformaldehyde (Sigma Aldrich, St Louis, MO) overnight and washed with successive dilutions of ethanol for thirty minutes. Scaffolds were washed twice with xylene and embedded in paraffin at 58°C . The paraffin block was sectioned using a manual rotary microtome (model RM 2125; Leica Biosystems, Buffalo Grove, IL). The sectioned scaffolds were deparaffinized and blocked using 10% species-appropriate serum in 3% glycine and PBS for 30 minutes before being stained. For both 1- and 2-color immunohistochemistry (IHC), the primary antibodies included mouse anti-Ki-67 (1:100 dilution; Biolegend), mouse anti-Isl-1 (Abcam), rabbit anti-vWF (Dako), and rabbit anti-TropT (Abcam). Incubation was performed at 4°C . Each section was washed with PBS/Tween 20, incubated with a secondary antibody for 1 hour at room temperature. For 1-color IHC, the secondary antibodies included goat anti-mouse PE (Southern Biotech, Birmingham, AL) or donkey anti-rabbit Alexa Fluor 647 (Life Technologies). For 2-color, the secondary antibodies included goat anti-mouse Alexa Fluor 488 (Life Technologies) or goat anti-rabbit Alexa Fluor 594 (Life Technologies). Slides were mounted in Prolong Gold with DAPI (Life Technologies). Sections were imaged using a LSM 710 NLO laser-scanning, confocal microscope (Carl Zeiss Microscopy GmbH, Jena, Germany) at a $20\times$ objective. Images were processed using ImageJ (v.1.49, NIH, <http://imagej.nih.gov/ij>).

Cell Proliferation and In Vivo Tracking

Cells were stained with CFSE (Biolegend), seeded onto the scaffold and cultured before IHC analysis (above).

TABLE 1.
Primers used for RT-PCR experiments

Human gene	Forward	Reverse
<i>β actin</i>	5'-TTTGAATGATGAGCCTTCGTCCCC-3'	5'-GGTCTCAAGTCAGTGTACAGGTAAGC-3'
<i>IGF-1</i>	5'-CAGAGCAGATAGAGCCTGCG-3'	5'-CAGGTAACCTCGTGACAGCA-3'
<i>HGF</i>	5'-CACGAACACAGCTTTTGGCC-3'	5'-TGATCCCAGCGGTGACAAAT-3'
<i>SDF-1α</i>	5'-CTACAGATGCCATGCCGAT-3'	5'-GTGGGTCTAGCGGAAAGTCC-3'
<i>Isl-1</i>	5'-CACAAAGCGTCTCGGGATTGTGTTT-3'	5'-AGTGGAAGTCTCCGACAA-3'
<i>c-Kit</i>	5'-ATTCCTCAAGCCATGAGTCTTGA-3'	5'-ACACGTGGAAACACCATCT-3'
<i>Bry</i>	5'-ACTGGATGAAGGCTCCCGTCTCCTT-3'	5'-CCAAGGCTGGACCAATTGTATGGG-3'
<i>Mesp-1</i>	5'-CGTATATCGGCCACCTGTC-3'	5'-GGCATCCAGGTCTCCAACAG-3'
<i>PDGFRα</i>	5'-GCGCAATCTGGACACTGGGA-3'	5'-ATGGGGTACTGCCAGCTCAC-3'
<i>TNNT2 (TropT)</i>	5'-GTGGGAAGAGGAGACTGAG-3'	5'-ATAGATGCTCTGCCACAGC-3'
<i>POU5F1 (OCT4)</i>	5'-AACCTGGAGTTGTGCCAGGGTT-3'	5'-TGAACCTCACCTCCCTCCAACCA-3'
<i>MLC2V</i>	5'-GGTGTGAAGGCTGATTACGTT-3'	5'-TATTGGAACATGGCCTCTGGAT-3'
Ovine gene		
<i>β actin</i>	5'-CGAGATGAGATTGGCCTCGT-3'	5'-CATGTTTGTAAAGGGCAGGA-3'
<i>Isl-1</i>	5'-GTGCAGCATCGGCTTCAGCAAAA-3'	5'-CCTCCCAGCGCGAAGTCT-3'
<i>c-Kit</i>	5'-GGCATATCCAAACCTGAACACCGA-3'	5'-CCCTGCGGCCACGCACTGTA-3'
<i>Bry</i>	5'-ACTGGATGAAGGCTCCCGTCTCCTT-3'	5'-CCAAGGCTGGACCAATTGTATGGG-3'

Statistical Analyses

For all normally distributed data, a 2-tailed, paired, Student *t* test was performed using Microsoft Excel. Statistical significance was assumed at $P < 0.05$. Data are represented as the mean \pm standard error.

RESULTS

CPCs Express Markers of Early Cardiogenic Mesoderm and Primordial Cardiovascular Progenitors

CPCs from human cardiac tissue were screened for the expression of early markers of cardiovascular differentiation. The phenotypic and functional characteristics of these cells were previously characterized.³ As shown in Figures 1A to C, CPC clones express markers of early cardiogenic mesoderm and primordial cardiovascular progenitors as well as display an ability to differentiate into cardiac derivatives (ie, cardiomyocytes, smooth muscle, and endothelium; Figure 1D). The expression of markers of early cardiogenic mesoderm was assessed using flow cytometry (Figures 1A-B) and by visualizing amplicons (Figure 1C). Gene expression analysis indicated the presence of *Mesp-1* and *brachyury (Bry)*; the robust coexpression of *Isl-1* and *c-kit*; and the expression of nascent cardiac progenitor markers, including *PDGFRα* and *KDR*. Taken together, this indicates that the CPCs used for experiments represent a state of development characteristic of early cardiogenic mesoderm and primordial cardiovascular progenitors (Figure 1E).

Patient-Derived CPCs Exhibit Markers of Pluripotency and Cardiac Derivatives on the Hyper-Crosslinked Carbohydrate Polymer Scaffold

We assessed the effect of scaffold culture on the maintenance of a CPC population (*Isl1*) and on the development of cardiomyocytes (*TropT*) and endothelial cells (*vWF*). Two- and 3-color FACS analysis indicated the expression of only *Isl1* under control culture conditions, but of *Isl1* along with *TropT* and *vWF* under scaffold culture conditions (Figures 2A-C). We confirmed the presence of cardiac derivatives by independently measuring

the protein expression of *TropT* and *vWF* using FACS analysis (Figure 2D, $n = 5$, $P < 0.001$). We then confirmed this concomitant maintenance of pluripotency and promotion of differentiation using RT-PCR, which indicated a significant 52-fold and 27-fold increase in the expression of *TNNT2* (*TropT*) and myosin regulatory light chain 2, ventricular isoform (*MLC2V*), respectively (Figure 2E, $n = 3$, $P < 0.001$). Similar to our findings by FACS analysis, we also identified a 70-fold increase in *POU5F1* (*OCT4*) expression (Figure 2E, $n = 3$, $P < 0.001$) and a 69-fold increase in *T* (*Bry*) expression (Figure 2E, $n = 3$, $P < 0.05$). To determine whether scaffold-cultured CPCs maintained their proliferative potential, we performed cell cycle analysis, which indicated a punctuated G1 phase (Figure 2F, $n = 3$, $P < 0.05$).

Scaffold Cultured CPCs Exhibit Autorhythmic Calcium Trafficking

After incubation with Fluo4-AM, a calcium dye, scaffold-cultured CPCs were imaged. Regions of interest were drawn around cells using ImageJ and the intensity of fluorescence in each region was quantified for each frame. As shown in Figure 3A, the scaffold-cultured CPCs exhibit an autorhythmic trafficking of calcium, which is a feature of mature cardiomyocytes, whereas flask-cultured CPCs do not ($n = 5-7$). Representative frames for sequential time points are shown for control and scaffold-cultured CPCs in Figures 3B and C, respectively.

ERK Activation Significantly Decreased While AKT Activation Increased in Scaffold-Cultured CPCs

We assessed changes in the activation of signaling molecules using flow cytometry to detect P-ERK and P-AKT. We observed a significant decrease in the number of P-ERK+ scaffold-cultured CPCs ($n = 4$, $P < 0.05$). We observed a general increase in P-AKT+ scaffold-cultured CPCs (Figures 4A-B).

Growth Factor and Chemokine Secretion Significantly Increased in Scaffold-Cultured Human CPCs

After the detection of significantly altered intracellular signaling cascades, we used RT-PCR to determine the level of expression of insulin-like growth factor 1 (*IGF-1*), hepatocyte

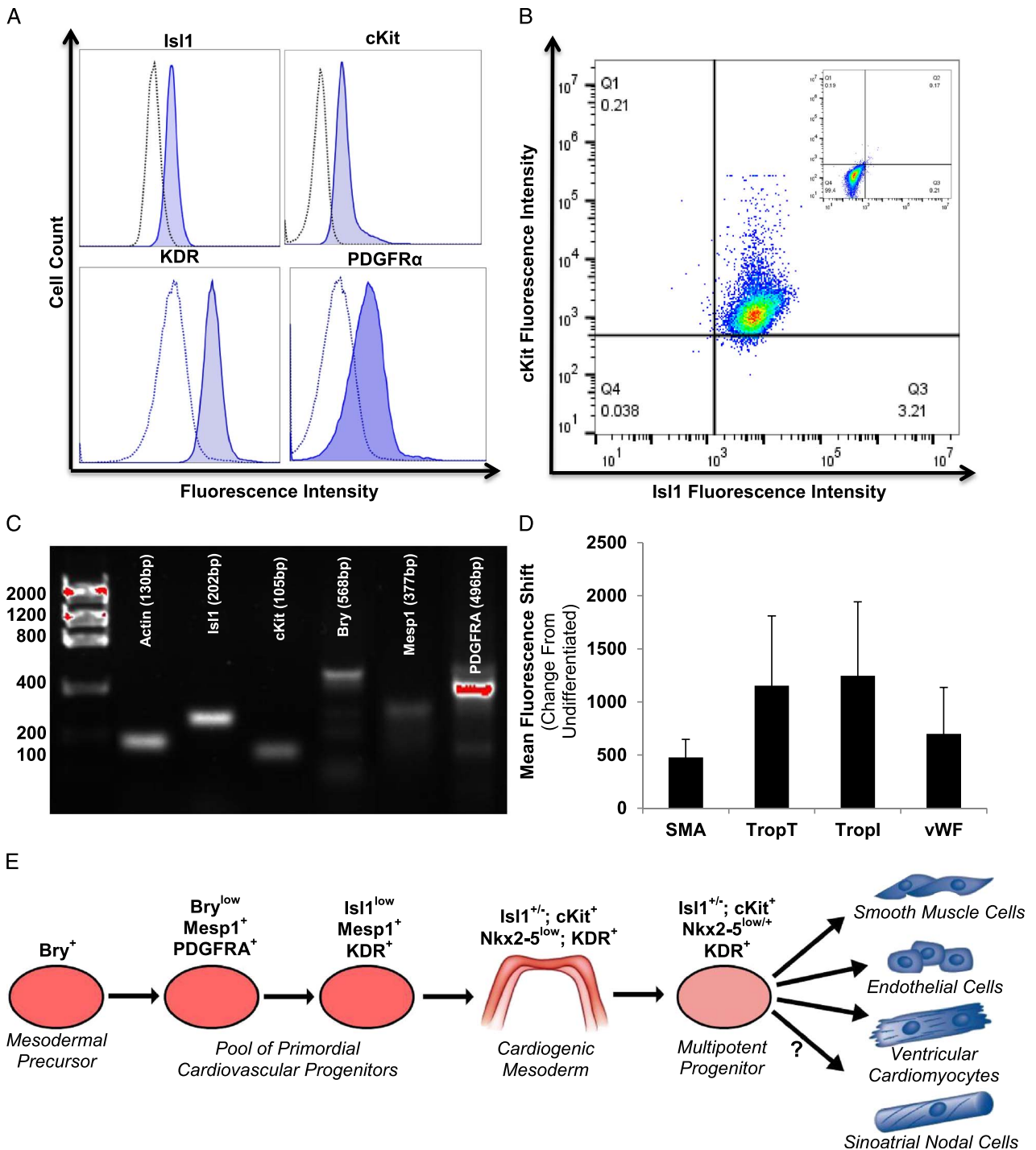


FIGURE 1. CPCs express markers of early cardiogenic mesoderm.³²⁻³⁶ CPCs used for experiments uniquely express markers of early cardiogenic mesoderm. The expression of markers of early cardiogenic mesoderm was assessed using flow cytometry (A-B). Notably, 2-color FACS analysis indicates the co-expression of Is1-1 and c-kit (B; negative population inset). We visualized amplicons of genes of interest using gel electrophoresis to verify this expression (C). CPCs express Mesp-1, Bry, Is1-1, c-kit, and PDGFR α . To confirm the multipotency of the CPCs, 10 nM of dexamethasone was used to induce the development of cardiomyocytes (TropT and TropI), endothelium (vWF), and smooth muscle (SMA). Antibodies against these proteins were measured using flow cytometry and reported as the change in mean fluorescence intensity compared with undifferentiated CPCs (D). As shown in panel E, mesoderm differentiates into cardiogenic mesoderm, which has the capacity to become several types of cardiac cells, including cardiomyocytes, endothelium, and smooth muscle. These human cardiac progenitors may give rise to sinoatrial nodal cells; however, the timing and location of specification is currently undetermined. Values represent the mean \pm S.E.M. n = 7.

growth factor (HGF), and stromal cell-derived factor 1 α (SDF-1 α) in scaffold-cultured and control CPCs. We found that the expression of both HGF and SDF-1 α was significantly

higher in the scaffold-cultured CPCs (Figures 5A-B, HGF: 48-fold increase, P value < 0.01; SDF-1 α : 77-fold increase; n = 3, P < 0.05).

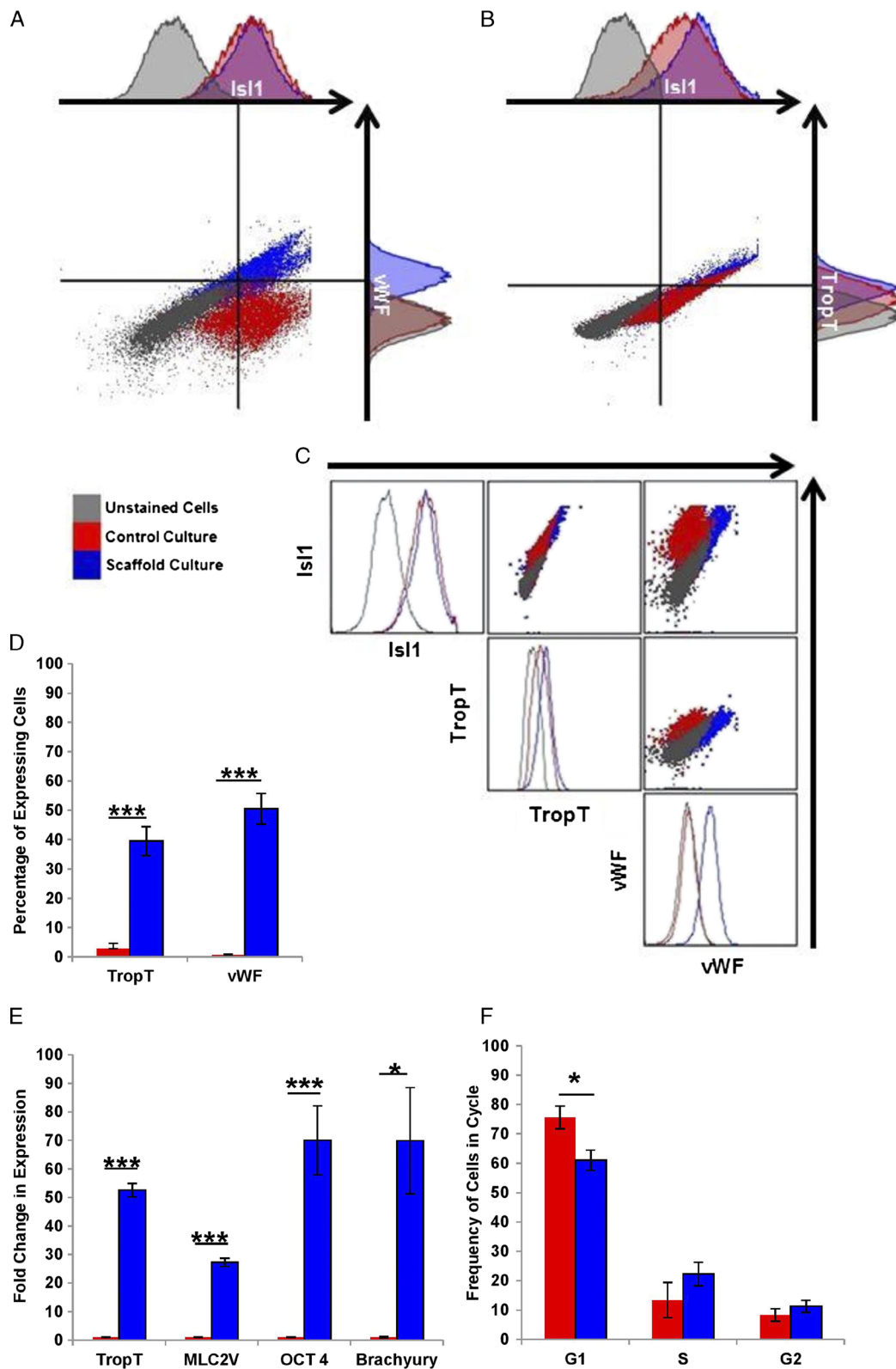


FIGURE 2. Scaffold-cultured CPCs exhibit a reduced G1 phase and markers of differentiation. Human-derived CPCs were scaffold-cultured. Two- and 3-color FACS analysis (A-C) indicated the expression of only Isl1 under control culture conditions (red), but of Isl1 along with TropT and vWF under scaffold culture conditions (blue). Populations were defined using unstained cells (grey). Flow cytometry verified the expression of TropT and vWF (D, $n = 5$, $P < 0.001$). RT-PCR indicated a significant 52-fold and 27-fold increase in the expression of *TNNI2* (TropT) and *MLC2V*, respectively (E, $n = 3$, $P < 0.001$). As indicated by FACS analysis, we also measured a 70-fold increase in *POU5F1* (OCT4) expression (E, $n = 3$, $P < 0.001$) and a 69-fold increase in *T* (Br) expression (E, $n = 3$, $P < 0.05$). To determine whether scaffold-cultured CPCs maintained their proliferative potential, we performed cell cycle analysis, which indicated a punctuated G1 phase (F, $n = 3$, $P < 0.05$). Mean values are reported, while error bars represent the S.E.M. * $P < 0.05$, $n = 3$; *** $P < 0.001$, $n = 4$.

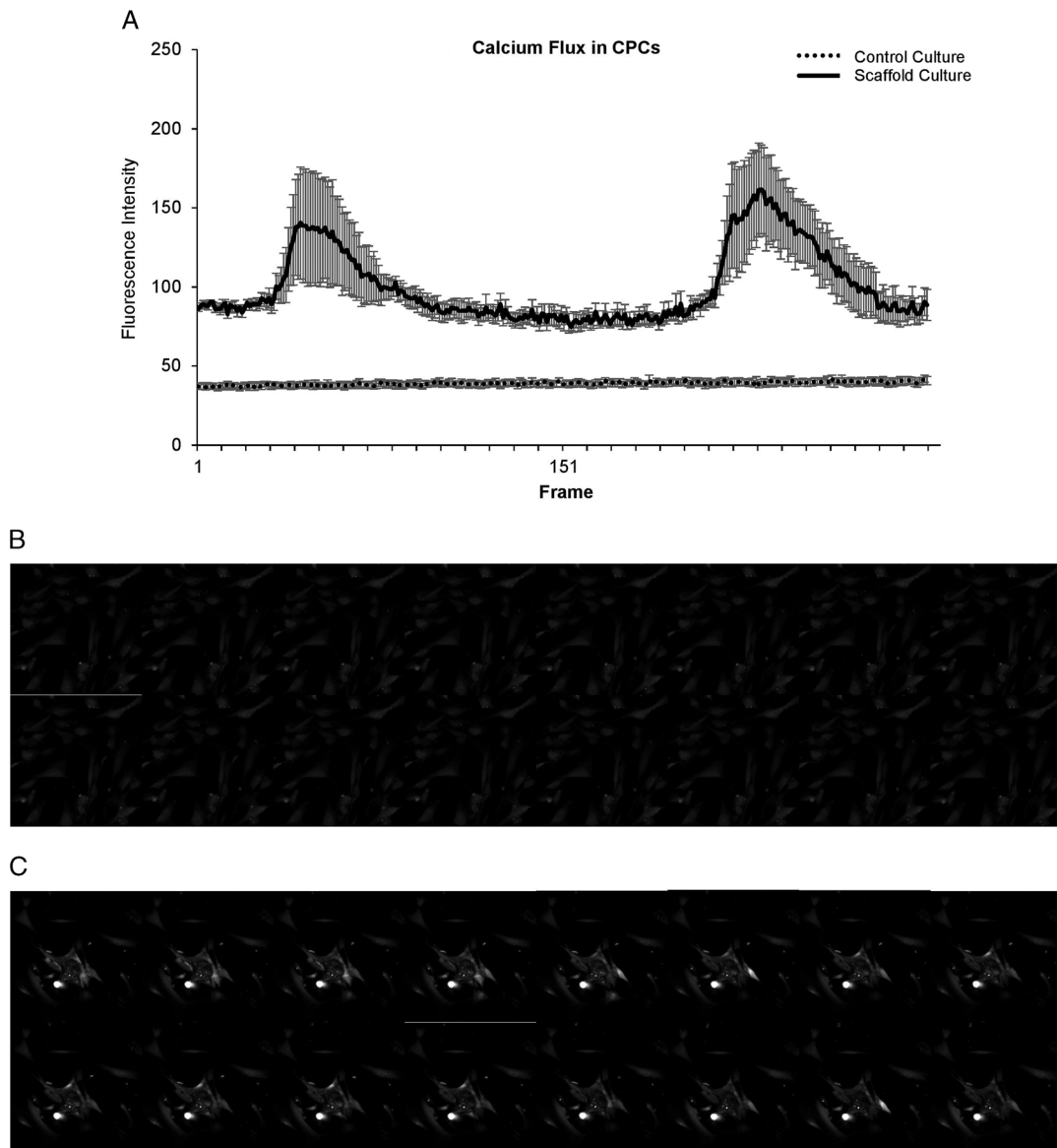


FIGURE 3. After scaffold culturing, cells display rhythmic pattern of calcium flux. After incubation with Fluo4-AM, a calcium dye, scaffold-cultured CPCs were imaged. Regions of interest were drawn around cells using ImageJ and the intensity of fluorescence in each region of interest was quantified for each frame. The scaffold-cultured CPCs exhibit an auto-rhythmic trafficking of calcium, which is a feature of mature cardiomyocytes, whereas control CPCs do not (A; $n = 5-7$). Representative frames for sequential time points are shown for control (B) and scaffold-cultured (C) CPCs.

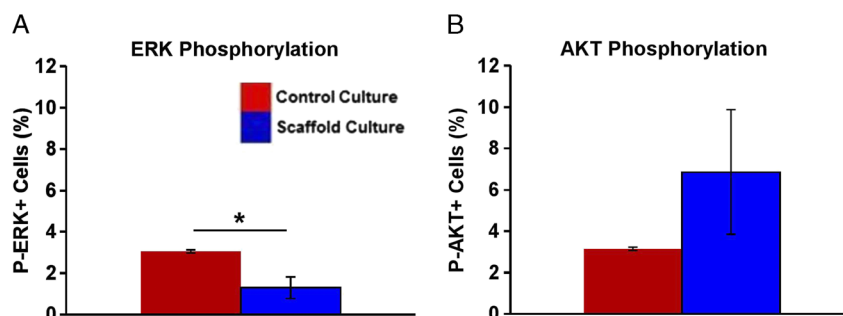


FIGURE 4. ERK phosphorylation decreases and AKT phosphorylation exhibits an increasing trend after scaffold culturing. Fluorophore-conjugated antibodies were used to detect the concentrations of (A) phosphorylated ERK1/2 (P-ERK+) and (B) phosphorylated AKT (P-AKT+) in cultured patient-derived CPCs. The phosphorylation of ERK1/2 was significantly reduced while the phosphorylation of AKT generally increased in the scaffold-cultured CPCs. Values represent the mean \pm SEM. * $P < 0.05$, $n = 4$.

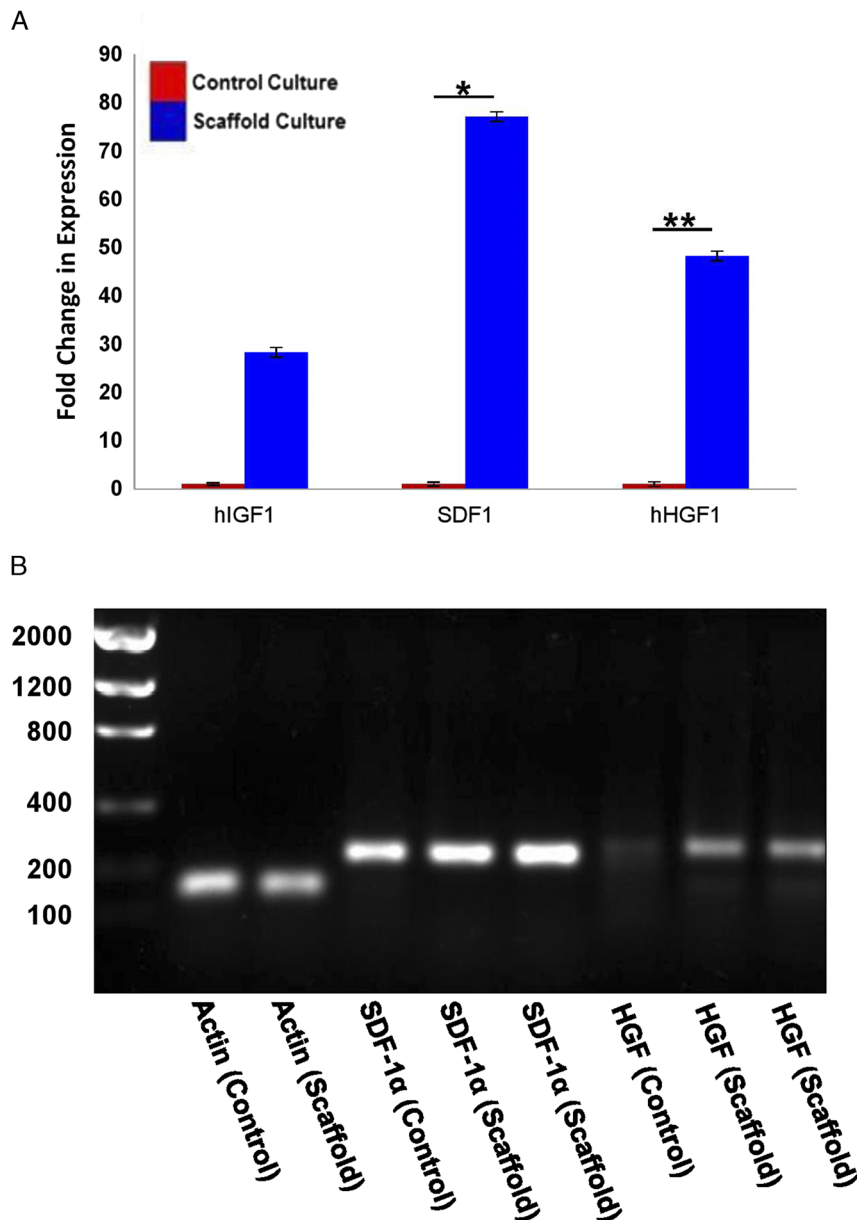


FIGURE 5. Scaffold-cultured progenitors show elevated expression of IGF-1, HGF, and SDF-1 α . The expression of cytokines in human CPCs was assessed after culturing under scaffold or control conditions (A). We confirmed the size of the statistically significant products from (A) using a 1% agarose gel (B). Band sizes based upon primer sequences: Actin (130 bp), SDF-1 α (226 bp), HGF (239 bp). * $P < 0.05$, ** $P < 0.01$, $n = 3$.

Ovine-Derived CPCs Express Markers of Early Cardiogenic Mesoderm and Primordial Cardiovascular Progenitors

CPCs were isolated from neonatal sheep in the same manner as the human CPCs.²⁸ Ovine-derived CPCs were previously characterized²⁸ and selected to express a similar pattern of markers that have been identified in human-derived CPCs. As shown in Figures 6A to B, these progenitor cell clones express the same markers that we identified in similarly isolated clones obtained from human patients. Ovine-derived CPCs express markers of early cardiogenic mesoderm and primordial cardiovascular progenitors. The expression of markers of early cardiogenic mesoderm was assessed by visualizing amplicons of genes of interest using gel electrophoresis (Figure 6A) and by flow cytometry (Figure 6B). Gene and

protein expression analysis indicates the presence of Bry, Isl-1 and c-kit in ovine CPCs.

Ovine-Derived, Scaffold-Cultured CPCs Express Increased Levels of the Differentiation Markers TropT and vWF

To develop an allogeneic model of early CPC transplantation on a scaffold in sheep using Isl-1 + c-kit + progenitor cells, we seeded scaffolds with ovine-derived Isl-1 + c-kit + CPC clones and cultured the scaffolds for 3 weeks, using the same procedures that we had used previously for culturing human-derived CPCs. We assessed the differentiation capacity of these cells using flow cytometry and IHC. Fluorophore-conjugated antibodies against the cardiomyocyte marker TropT and endothelial marker vWF were used to detect the presence of

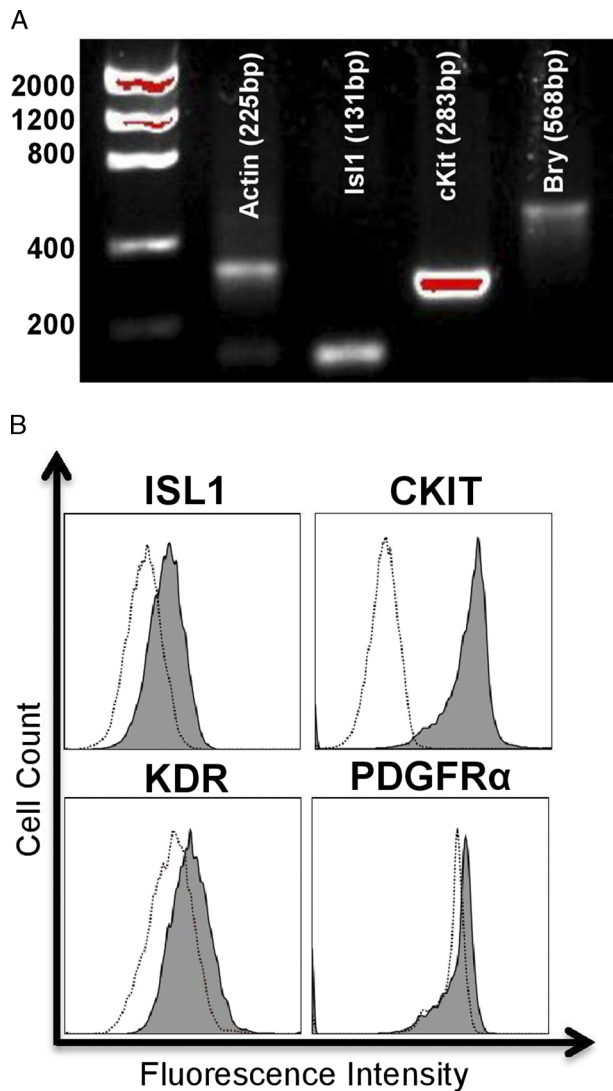


FIGURE 6. Ovine-derived CPCs express markers of early cardiogenic mesoderm. The expression of markers of early cardiogenic mesoderm was assessed by visualizing amplicons of genes of interest using gel electrophoresis (A) and by flow cytometry (B). Similar to the profile of human-derived CPCs, gene and protein expression analysis indicates the presence of Bry, Isl-1, and c-kit in ovine CPCs.

differentiated cells using flow cytometry. Scaffold-cultured, ovine-derived CPCs express increased levels of TropT (Figure 7A) and significantly increased levels of vWF (Figure 7D, $n = 3$, $P < 0.001$). This protein expression in scaffold-cultured CPCs was confirmed by confocal microscopy, in which the expression of both TropT and vWF are observed in the scaffold-cultured cell populations (Figures 7B-C and E-F).

Ovine-Derived, Scaffold-Cultured CPCs Express Increased Levels of Isl-1 and Ki-67 as Well as a Prostem Cell Shift in Cell Cycling

We sought to determine whether the differentiation observed in ovine-derived CPC scaffold culture would be paired with the maintenance of pluripotency, similar to our observations using human patient-derived CPC. We assessed the nature of the retained pluripotency markers by examining Isl-1 expression using RT-PCR and IHC. *ISL-1* expression, a marker of cardiogenic stemness, was significantly elevated 5.6-fold ($n = 3$,

$P < 0.05$, Figure 7G). This gene expression was preserved at the protein level, as indicated by the presence of Isl-1 staining (Figures 7H-I). We observed a prostem cell shift in the cell cycle profile of scaffold-cultured ovine CPCs using flow cytometry (Figure 7J). Scaffold-cultured ovine CPCs stained for Ki-67, a marker of proliferation (Figures 7K-L).

Ovine- and Human-Derived, Scaffold-Cultured CPCs Concomitantly Express Isl1, TropT, and vWF

To validate the presence of cardiac derivatives and progenitors within scaffold-cultured ovine CPCs, we performed FACS analysis using antibodies against Isl1, TropT, and vWF (Figures 8A-C). We observed the expression of all 3 markers under scaffold conditions, but of only Isl1 under control culture conditions. This was then confirmed by IHC analysis on serial sections of paraffin-embedded scaffolds that were seeded with ovine-derived CPCs (Figures 8D-F).

DISCUSSION

Stem cell-based therapies remain limited in efficacy, in part due to the ongoing challenge of poor cell retention at the site of damage. We have demonstrated here that Isl-1 + c-kit + CPCs cultured on a hyper-crosslinked carbohydrate polymer scaffold proliferate, retain a CPC reserve within the scaffold, and differentiate into cardiomyocytes and endothelial cells, providing a niche that may be useful in future studies of cardiovascular transplantation and eventual clinical application.

Clinical regeneration is predicated, in part, by suitable pre-clinical studies. Because the ovine heart is similar to the human heart,^{25,28} the ovine model has become an accepted large animal model for cardiac research.²⁶ The similar profile of gene and protein expression in human- and ovine-derived CPCs, as well as the similar results obtained after scaffold culture, suggest a plausible path forward for allogeneic pre-clinical modeling of cardiac repair. Many limiting factors require optimization to improve cell-based repair, which can be addressed using scaffold-based culture of sheep progenitor cells for transplantation.

Previous efforts to optimize scaffold culture conditions to produce an appropriate ratio of cardiac derivatives for transplantation with the capability of repairing the damaged myocardium and providing vascularization to the site of damage are ongoing.^{16,17,21-23,38} We conducted our experiments using early stage cardiovascular committed CPCs with the objective of providing a progenitor with the capability of differentiating into all cardiovascular lineages on the scaffold, consistent with the differentiation capability of these cells when induced in vivo. Induction of endothelial and cardiomyocyte marker expression was paired with the maintenance of pluripotent markers and a prostemness cell cycle profile. We observed a statistically significant reduction in the G1 phase of the human-derived, scaffold-cultured CPCs. This punctuation of the G1 phase is characteristic of stem cell cycling.^{39,40} This observation, along with the increase in cardiac derivative marker expression, suggests that a portion of the CPCs cultured using a scaffold experienced both a punctuated G1 phase and increased pluripotency markers that are characteristic of proliferative stem cells, whereas other CPCs differentiated. This was supported by the expression of Isl-1 and Ki-67 in ovine-derived scaffold cultures. Consistent with this concept, a biomimetic hydrogel scaffold was previously shown to provide a functional niche in which

stemness was promoted through the expression of self-renewal-associated transcription factors.⁴¹ Other biomaterial substrates have also been reported to foster the spontaneous formation of cellular spheroids, which preserve stemness.⁴²

In addition to preserving proliferative potential, a 3D-printed/hyaluronic acid matrix containing CPCs preserved their ability to subsequently differentiate using 5-Azacytidine.³⁷ Similarly, we show that stemness can be preserved on an 8 ×

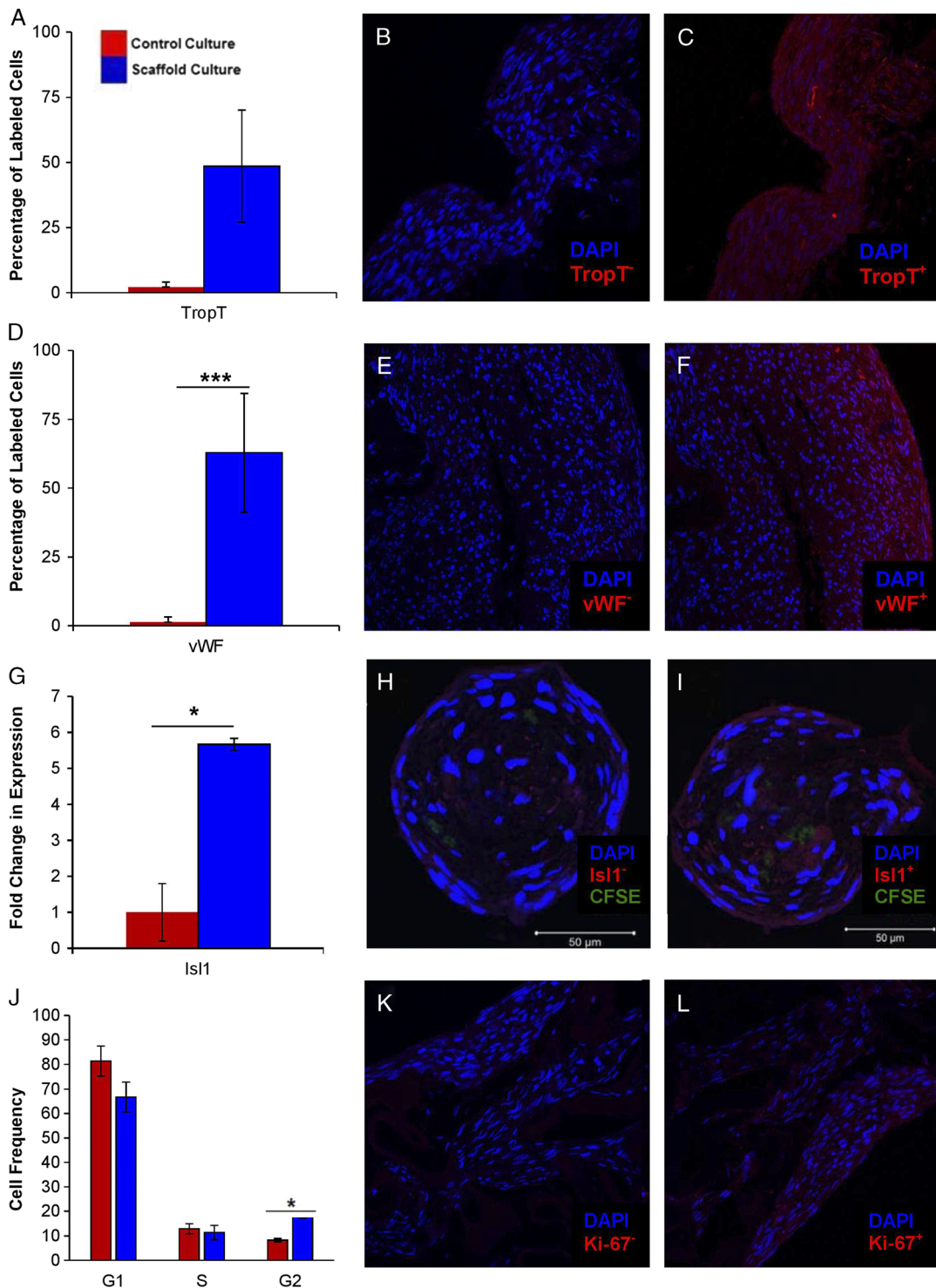


FIGURE 7. Scaffold-cultured, ovine-derived CPCs maintain proliferative and stem-like potential while differentiating into cardiac derivatives. Using genetic and protein expression analysis, we measured the coexistence of differentiating and proliferating stem cells. FACS analysis and IHC were used to assess the expression of TropT and vWF. Scaffold-cultured, ovine-derived CPCs express increased levels of TropT (A-C) and significantly increased levels of vWF (D-F). RT-PCR and flow cytometry indicated the increased expression of IsI1 (G-I). Flow cytometry indicated a prostem cell shift in the cell cycle profile of scaffold-cultured ovine CPCs (J). Scaffold-cultured ovine CPCs stained positively for Ki-67, a marker of proliferation (K-L).³⁷ Interestingly, the scaffold culture of CPCs induced differentiation yet a proportion of cells were maintained that express the stem cell marker IsI-1. * $P < 0.05$, $n = 3$; *** $P < 0.001$, $n = 3$.

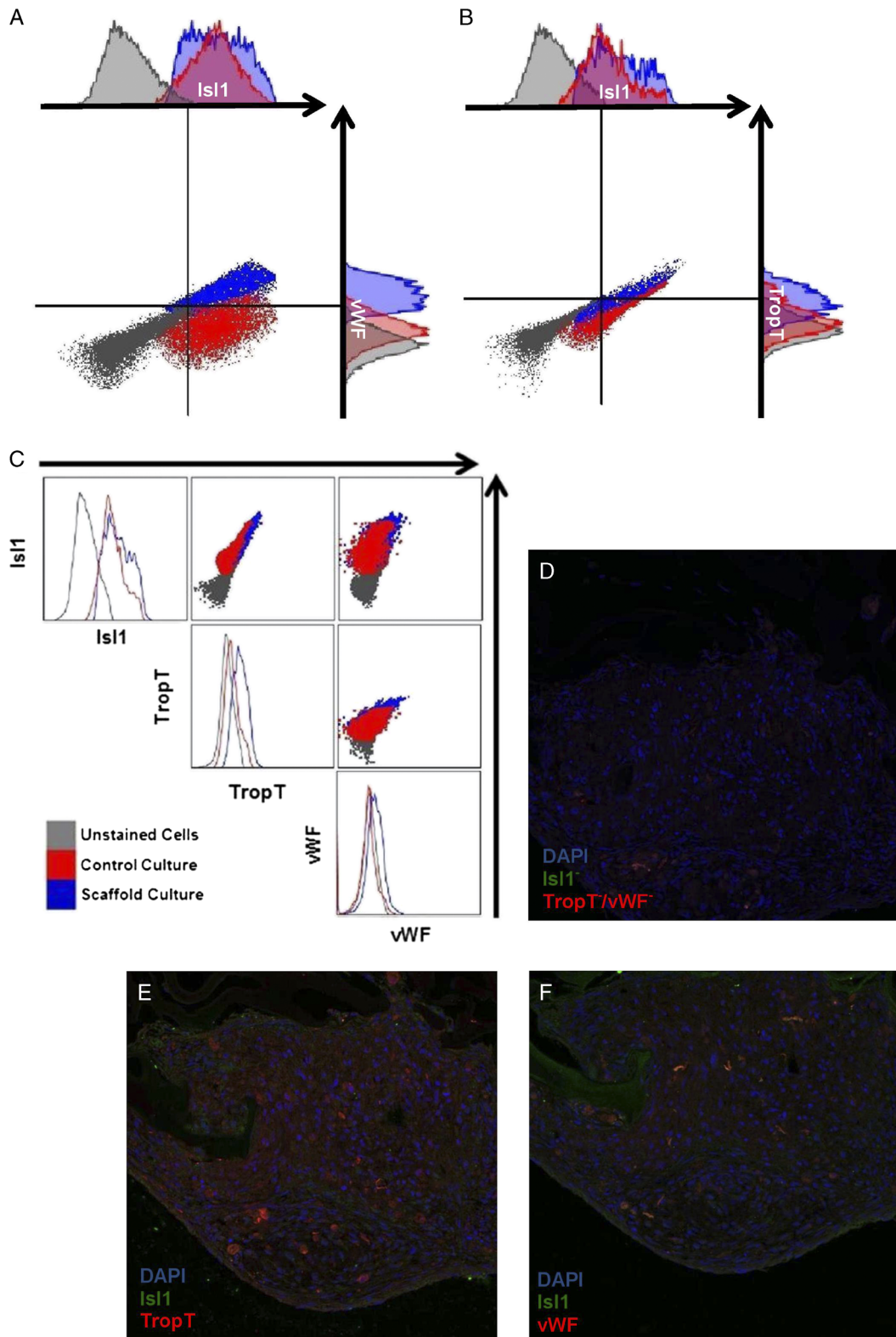


FIGURE 8. Concomitant expression of Isl1, TropT, and vWF in ovine-derived, scaffold-cultured CPCs. In an effort to clarify the presence of both cardiac progenitor and derivative markers, we performed FACS analysis of CPCs cultured for 3 weeks under control (red) and scaffold (blue) conditions (A-C). Unlike control conditions, under which CPCs expressed only Isl1, scaffold conditions fostered both the maintenance of Isl1 as well as the expression of vWF (A) and TropT (B). Unstained cells are shown in grey. To confirm these observations, we performed IHC analysis of serial sections of paraffin-embedded scaffolds that were seeded with ovine-derived CPCs. Secondary only staining is shown in (D). Isl1 and TropT (E) as well as Isl1 and vWF (F) were all observed to be concomitantly expressed.

2 mm hyper-crosslinked polymer scaffold of 97% porosity (20–80 μm pore size). Yet, we also demonstrated that this proliferative potential of CPCs is maintained in conjunction with differentiation in the absence of exogenous factors after scaffold culture. Using FACS and IHC analysis of scaffold-cultured CPCs derived from both human and ovine sources, we observed the concomitant expression of the progenitor marker Isl1 and the derivative markers TropT and vWF. This maintenance of a reserve pool of progenitors along with differentiation is perhaps a consequence of the unique progenitor cell/scaffold pairing in the model presented herein.

Scaffolds work through their mechanical properties and topography to partly direct cells towards differentiation or “dedifferentiation” (ie, the loss of a differentiated phenotype).⁴³ This logically follows from the resemblance of the 3D scaffold structure to the stem cell niches that are endogenous to the human body and can facilitate the ECM remodeling that is necessary to address the needs of development.^{44–46} A 3D environment recreates the physical interactions⁴² that affect the migration,⁴⁷ proliferation,⁴⁸ and apoptosis⁴⁹ of stem cells. We observed differentiation in the scaffold-cultured population in both human- and ovine-derived CPCs and an induction of autorhythmic calcium flux in scaffold-culture CPCs that was nonexistent in control cultures. A recent report identified that the mechanical stress of a 3D environment favors cardiac-specific derivatives of induced pluripotent stem cells (iPSCs).⁵⁰ This differentiation of CPCs towards the cardiomyocyte lineage is restricted by a maximal pressure exerted (ie, “stiffness”) by the ECM.⁵¹ Differentiation is commonly observed in stem cells that are cultured using ECM-like conditions¹² or when used in a fibrin enriched environment.^{52,53}

Differentiation is a consequence of scaffold-cultured stem cell interaction with the ECM.¹³ We therefore explored the regulatory signaling pathway and chemokine expression profile of scaffold-cultured CPCs in our model. We observed a decline in MEK/ERK signaling but a trend toward elevated PI3K/AKT phosphorylation. This is consistent with previous reports in which AKT signaling and ERK suppression is evidenced to preserve stemness,^{54–57} particularly in scaffold-cultured stem cells.⁵⁸ Changes in ERK1/2 activity have been documented to be involved in the conversion of pluripotent stem cells to committed cell lineages.⁵⁷ Interestingly, reducing β catenin signaling, as is the case in reduced ERK signaling,^{59,60} facilitates the respecification of cranial mesoderm into cardiomyocytes.⁶¹

Scaffolds that support the maintenance of stem cells solely for the purpose of paracrine factor secretion have provided beneficial effects after transplantation.⁶² Paracrine factors enhance neovascularization and reduce cell death. Recently, a swine model of an acute myocardial infarction demonstrated improved clinical outcomes after IGF-1 and HGF administration⁶³ due to a reduction in pathologic tissue growth (fibroblast proliferation) and an induction of myocardial regeneration. SDF-1 α , an angiogenic factor, has been shown to be beneficial in numerous transplant and basic science settings.^{11,63–67} Among these, Tilokee et al⁶⁵ have shown that the paracrine effect of CPC transplantation itself is sufficient to promote cardiac repair. In addition to our observations, these studies have shown that a stem cell/scaffold combination has the potential to mobilize and recruit stem cells due to the presence of growth factor receptor systems that mobilize CPCs and support myocardial regeneration.

Preclinical studies that assess this capability and the capacity of the reserve progenitor population to contribute to regeneration in vivo will be necessary to verify whether these findings benefit functional outcomes in the field of stem cell transplantation.

ACKNOWLEDGMENTS

Confocal microscopy was performed at the Loma Linda University Advanced Imaging and Microscopy Core with support from the National Science Foundation under Major Research Instrumentation, Division of Biological Infrastructure grant 0923559 (SM Wilson) and Loma Linda University School of Medicine.

REFERENCES

- Behfar A, Crespo-Diaz R, Terzic A, et al. Cell therapy for cardiac repair—lessons from clinical trials. *Nat Rev Cardiol*. 2014;11:232–246.
- Daley GQ. The promise and perils of stem cell therapeutics. *Cell Stem Cell*. 2012;10:740–749.
- Fuentes TI, Appleby N, Tsay E, et al. Human neonatal cardiovascular progenitors: unlocking the secret to regenerative ability. *PLoS One*. 2013;8:e77464.
- Askari AT, Unzek S, Popovic ZB, et al. Effect of stromal-cell-derived factor 1 on stem-cell homing and tissue regeneration in ischaemic cardiomyopathy. *Lancet*. 2003;362:697–703.
- Beltrami AP, Barlucchi L, Torella D, et al. Adult cardiac stem cells are multipotent and support myocardial regeneration. *Cell*. 2003;114:763–776.
- Pittenger MF, Mackay AM, Beck SC, et al. Multilineage potential of adult human mesenchymal stem cells. *Science*. 1999;284:143–147.
- Matsuura K, Nagai T, Nishigaki N, et al. Adult cardiac Sca-1-positive cells differentiate into beating cardiomyocytes. *J Biol Chem*. 2004;279:11384–11391.
- Ellison GM, Vicinanza C, Smith AJ, et al. Adult c-kit(pos) cardiac stem cells are necessary and sufficient for functional cardiac regeneration and repair. *Cell*. 2003;154:827–842.
- Anversa P, Kajstura J, Rota M, et al. Regenerating new heart with stem cells. *J Clin Invest*. 2013;123:62–70.
- Chong JJ, Yang X, Don CW, et al. Human embryonic-stem-cell-derived cardiomyocytes regenerate non-human primate hearts. *Nature*. 2014;510:273–277.
- Godier-Furnémont AF, Martens TP, Koeckert MS, et al. Composite scaffold provides a cell delivery platform for cardiovascular repair. *Proc Natl Acad Sci U S A*. 2011;108:7974–7979.
- Sreejit P, Verma RS. Natural ECM as biomaterial for scaffold based cardiac regeneration using adult bone marrow derived stem cells. *Stem Cell Rev*. 2013;9:158–171.
- Leor J, Amsalem Y, Cohen S. Cells, scaffolds, and molecules for myocardial tissue engineering. *Pharmacol Ther*. 2005;105:151–163.
- Gaetani R, Doevendans PA, Metz CH, et al. Cardiac tissue engineering using tissue printing technology and human cardiac progenitor cells. *Biomaterials*. 2012;33:1782–1790.
- Maher B. Tissue engineering: how to build a heart. *Nature*. 2013;499:20–22.
- Murry C, Soonpaa M, Reinecke H, et al. Haematopoietic stem cells do not transdifferentiate into cardiac myocytes in myocardial infarcts. *Nature*. 2004;428:664–668.
- Balsam LB, Wagers AJ, Christensen JL, et al. Haematopoietic stem cells adopt mature haematopoietic fates in ischaemic myocardium. *Nature*. 2004;428:668–673.
- Dixon J, Gorman R, Stroud R, et al. Mesenchymal cell transplantation and myocardial remodeling after myocardial infarction. *Circulation*. 2009;120:S220–S229.
- Segers VF, Lee RT. Stem-cell therapy for cardiac disease. *Nature*. 2008;451:937–942.
- Dubois C, Liu X, Claus P, et al. Differential effects of progenitor cell populations on left ventricular remodeling and myocardial neovascularization after myocardial infarction. *J Am Coll Cardiol*. 2010;55:2232–2243.
- Beitnes JO, Hopp E, Lunde K, et al. Long-term results after intracoronary injection of autologous mononuclear bone marrow cells in acute myocardial infarction: the ASTAMI randomised, controlled study. *Heart*. 2009;95:1983–1993.

22. Lafflamme MA, Murry CE. Regenerating the heart. *Nat Biotechnol*. 2005; 23:845–856.
23. Dar A, Shachar M, Leor J, et al. Optimization of cardiac cell seeding and distribution in 3D porous alginate scaffolds. *Biotechnol Bioeng*. 2002;80: 305–312.
24. Meng X, Leslie P, Zhang Y, et al. Stem cells in a three-dimensional scaffold environment. *Springerplus*. 2014;3:80.
25. Gorman JH 3rd, Gorman RC, Plappert T, et al. Infarct size and location determine development of mitral regurgitation in the sheep model. *J Thorac Cardiovasc Surg*. 1998;115:615–622.
26. Dixon JA, Spinale FG. Development of therapeutics for heart failure: large animal models of heart failure. *Circ Heart Fail*. 2009;2:262–271.
27. Fuentes TI, Appleby N, Raya M, et al. Simulated microgravity exerts an age-dependent effect on the differentiation of cardiovascular progenitors isolated from the human heart. *PLoS One*. 2015;10:e0132378.
28. Hou X, Appleby N, Fuentes T, et al. Isolation, characterization, and spatial distribution of cardiac progenitor cells in the sheep heart. *J Clin Exp Cardiol*. 2012;(Suppl 6):004.
29. Krutzik PO, Nolan GP. Intracellular phospho-protein staining techniques for flow cytometry: monitoring single cell signaling events. *Cytometry A*. 2013;55:61–70.
30. Abrahamsen I, Lorens JB. Evaluating extracellular matrix influence on adherent cell signaling by cold trypsin phosphorylation-specific flow cytometry. *BMC Cell Biol*. 2013;14:36.
31. Jun HS, Lee YM, Song KD, et al. G-CSF improves murine G6PC3-deficient neutrophil function by modulating apoptosis and energy homeostasis. *Blood*. 2014;117:3881–3892.
32. Kataoka H, Takakura N, Nishikawa S, et al. Expressions of PDGF receptor alpha, c-Kit and Flk1 genes clustering in mouse chromosome 5 define distinct subsets of nascent mesodermal cells. *Dev Growth Differ*. 1997;9: 729–740.
33. Martin-Puig S, Wang Z, Chien KR. Lives of a heart cell: tracing the origins of cardiac progenitors. *Cell Stem Cell*. 2008;2:320–331.
34. Moretti A, Caron L, Nakano A, et al. Multipotent embryonic isl1+ progenitor cells lead to cardiac, smooth muscle, and endothelial cell diversification. *Cell*. 2006;127:1151–1165.
35. Soriano P. The PDGF alpha receptor is required for neural crest cell development and for normal patterning of the somites. *Development*. 1997; 124:2691–2700.
36. Yang L, Soonpaa MH, Adler ED, et al. Human cardiovascular progenitor cells develop from a KDR+ embryonic-stem-cell-derived population. *Nature*. 2008;453:524–528.
37. Scholzen T, Gerdes J. The Ki-67 protein: from the known and the unknown. *J Cell Physiol*. 2000;182:311–322.
38. Gaetani R, Feyen DA, Verhage V, et al. Epicardial application of cardiac progenitor cells in a 3D-printed gelatin/hyaluronic acid patch preserves cardiac function after myocardial infarction. *Biomaterials*. 2015;61: 339–348.
39. Becker KA, Ghule PN, Therrien JA, et al. Self-renewal of human embryonic stem cells is supported by a shortened G1 cell cycle phase. *J Cell Physiol*. 2006;209:883–893.
40. White J, Dalton S. Cell cycle control of embryonic stem cells. *Stem Cell Rev*. 2005;1:131–138.
41. Rustad KC, Wong VW, Sorkin M, et al. Enhancement of mesenchymal stem cell angiogenic capacity and stemness by a biomimetic hydrogel scaffold. *Biomaterials*. 2012;33:80–90.
42. Huang GS, Dai LG, Yen BL, et al. Spheroid formation of mesenchymal stem cells on chitosan and chitosan-hyaluronan membranes. *Biomaterials*. 2011;32:6929–6945.
43. Guilak F, Cohen DM, Estes BT, et al. Control of stem cell fate by physical interactions with the extracellular matrix. *Cell Stem Cell*. 2009;5:17–26.
44. Scadden DT. The stem-cell niche as an entity of action. *Nature*. 2006;441: 1075–1079.
45. Levenberg S, Huang NF, Lavik E, et al. Differentiation of human embryonic stem cells on three-dimensional polymer scaffolds. *Proc Natl Acad Sci U S A*. 2003;100:12741–12746.
46. Daley WP, Peters SB, Larsen M. Extracellular matrix dynamics in development and regenerative medicine. *J Cell Sci*. 2008;121:155–164.
47. Guo WH, Frey MT, Burnham NA, et al. Substrate rigidity regulates the formation and maintenance of tissues. *Biophys J*. 2006;90:2213–2220.
48. Hadjipanayi E, Mudera V, Brown RA. Close dependence of fibroblast proliferation on collagen scaffold matrix stiffness. *J Tissue Eng Regen Med*. 2009;3:77–84.
49. Wang HB, Dembo M, Wang YL. Substrate flexibility regulates growth and apoptosis of normal but not transformed cells. *Am J Physiol Cell Physiol*. 2000;279:C1345–C1350.
50. Ruan JL, Tulloch NL, Saiget M, et al. Mechanical stress promotes maturation of human myocardium from pluripotent stem cell-derived progenitors. *Stem Cells*. 2015;33:2148–2157.
51. Forte G, Carotenuto F, Pagliari F, et al. Criticality of the biological and physical stimuli array inducing resident cardiac stem cell determination. *Stem Cells*. 2008;26:2093–2103.
52. Christman KL, Fok HH, Sievers RE, et al. Fibrin glue alone and skeletal myoblasts in a fibrin scaffold preserve cardiac function after myocardial infarction. *Tissue Eng*. 2004;10:403–409.
53. Bellamy V, Vanneaux V, Bel A, et al. Long-term functional benefits of human embryonic stem cell-derived cardiac progenitors embedded into a fibrin scaffold. *J Heart Lung Transplant*. 2015;34:1198–1207.
54. Watanabe S, Umehara H, Murayama K, et al. Activation of Akt signaling is sufficient to maintain pluripotency in mouse and primate embryonic stem cells. *Oncogene*. 2006;25:2697–2707.
55. Burdon T, Tracey C, Chambers I, et al. Suppression of SHP-2 and ERK signalling promotes self-renewal of mouse embryonic stem cells. *Dev Biol*. 1999;210:30–43.
56. Ying QL, Wray J, Nichols J, et al. The ground state of embryonic stem cell self-renewal. *Nature*. 2008;452:519–523.
57. Kunath T, Saba-El-Leil MK, Almousailleakh M, et al. FGF stimulation of the Erk1/2 signalling cascade triggers transition of pluripotent embryonic stem cells from self-renewal to lineage commitment. *Development*. 2007;134: 2895–2902.
58. Nur-E-Kamal A, Ahmed I, Kamal J, et al. Three-dimensional nanofibrillar surfaces promote self-renewal in mouse embryonic stem cells. *Stem Cells*. 2006;24:426–433.
59. Yamaguchi H, Hsu JL, Hung MC. Regulation of ubiquitination-mediated protein degradation by survival kinases in cancer. *Front Oncol*. 2012;2:15.
60. Ding Q, Xia W, Liu JC, et al. Erk associates with and primes GSK-3beta for its inactivation resulting in upregulation of beta-catenin. *Mol Cell*. 2005;19: 159–170.
61. Palpant NJ, Pabon L, Roberts M, et al. Inhibition of β -catenin signaling respecifies anterior-like endothelium into beating human cardiomyocytes. *Development*. 2015;142:3198–3209.
62. Naderi-Meshkin H, Matin MM, Heirani-Tabasi A, et al. Injectable hydrogel delivery plus preconditioning of mesenchymal stem cells: exploitation of SDF-1/CXCR4 axis toward enhancing the efficacy of stem cells' homing. *Cell Biol Int*. 2016;40:730–741.
63. Ellison GM, Torella D, DelleGrottaglie S, et al. Endogenous cardiac stem cell activation by insulin-like growth factor-1/hepatocyte growth factor intracoronary injection fosters survival and regeneration of the infarcted pig heart. *J Am Coll Cardiol*. 2011;58:977–986.
64. Engler AJ, Sen S, Sweeney HL, et al. Matrix elasticity directs stem cell lineage specification. *Cell*. 2006;126:677–689.
65. Tilokee EL, Latham N, Jackons R, et al. Paracrine engineering of human explant-derived cardiac stem cells to over-express stromal-cell derived factor 1 α enhances myocardial repair. *Stem Cells*. 2016;34:1826–1835.
66. Zhang G, Nakamura Y, Wang X, et al. Controlled release of stromal cell-derived factor-1 alpha in situ increases c-kit + cell homing to the infarcted heart. *Tissue Eng*. 2007;13:2063–2071.
67. Urbaneck K, Rota M, Cascapera S, et al. Cardiac stem cells possess growth factor-receptor systems that after activation regenerate the infarcted myocardium, improving ventricular function and long-term survival. *Circ Res*. 2005;97:663–673.